Int. J. Electrochem. Sci., 15 **(2020)** 2115 – 2132, doi: 10.20964/2020.03.69

International Journal of ELECTROCHEMICAL SCIENCE
www.electrochemsci.org

Review

Oxidation and Deformation behaviours of the 316L Stainless-Steel Weldments in Nuclear Plants

Hassan Tukur[*], *Lu Yonghao*[*]

National Center for Material Service Safety, University of Science and Technology, Beijing,
[*]E-mail: tingilin@yahoo.com, lu_yonghao@mater.edu.cn

Received: 9 November 2019 / *Accepted:* 13 January 2020 / *Published:* 10 February 2020

As an essential component in nuclear power plants, which is an important means to solve the global energy crises, the safety of heterogeneous metal welding joints in the main pipelines is very critical. Therefore, to prolong the life of welding joints and improve safety of nuclear power plants, it is of great significance to study the structure of dissimilar metal welding parts and its influence on the deformation behavior of welding parts at room temperature and the oxidation behavior and mechanism of water at high temperature. In this paper, a review of studies on the safety end of 316L stainless-steel/Inconel dissimilar welding as used in nuclear power plants is presented. The weld microstructure and corrosion properties at room temperature and high temperature water oxidation behavior, studied by means of optical microscope, Scanning Electron Microscope (SEM), X-ray photoelectron spectroscopy and Transmission Electron Microscopy (TEM), on the sample of the welding parts were presented and analyzed. Also, studies using the in-situ tensile technique to investigate the influence of microstructure evolution in microstructure crack initiation and propagation, as well as the microstructure evolution rule of welded parts during tensile process were reviewed in detail. The correlation between the articles on microstructure and deformation were analyzed and all the shortcomings were highlighted with suggestions for further research.

Keywords: Dissimilar Metal, Fusion Zone, Weld Corrosion, Residual Stress

1. INTRODUCTION

The main materials used in the main equipment of large nuclear power plants in the world are mainly austenitic stainless-steel and nickel-based alloy, and the main types of austenitic stainless steel are 304L and 316L [1-3]. According to the actual service conditions of pressurized water reactor, mostly with 300 series austenitic stainless-steel, mainly divided into the following three [7]; the first type for stabilizing austenitic stainless-steel such as 321 steel (09 x18h10t). They are in the original [18-8] austenitic stainless-steel with Ti and Nb. They enhance the inter-granular corrosion resistance of stainless-steel but reduce the welding performance and production difficulty. The second is the

standard 304L (0 cr18ni9) and 316L (0 cr17ni12mo2) type of austenitic stainless-steel. They stay in between 480℃ to 820℃ for a long time and the grain boundary carbide precipitation tendency usually happens to be "sensitive". The third type is ultra-low carbon austenitic stainless-steel 304L (00Cr19Ni10) and 316L (00Cr17Ni14Mo2), which further reduces the carbon content on the basis of 304L and 316L. In addition to primary main pipelines, 304L and 316L austenitic steels are also widely used as structural materials for important components such as pile internals and driving mechanisms. Since the thermal expansion coefficient of nickel-based alloy is close to that of austenitic steel and ferrite steel, it can effectively curb the carbon diffusion at the weld interface and form heterogeneous steel welded joints with stable structure. So, nickel-based alloy is mostly used as the filler material for welding parts

2. METHODOLOGY

We systematically reviewed papers from 2004 to date and examine the literatures on issues relating to use of stainless-steel in nuclear plants. Data collected from Science Direct, Web of Science, Google Scholar, Scopus and ResearchGate were utilized. Databases where broadly searched focusing on different topics and sub-topics namely; material science and failure characteristics of heterogeneous welded joints, dissimilar metal welded joints, microstructure dissimilar metal welded joints, residual stress of dissimilar metal welded joints, mechanical properties of heterogeneous metal welding, corrosion performance of stainless-steel welding parts, uniform corrosion, pitting, intergranular corrosion, stress corrosion, corrosion product films in high-temperature and high-pressure water environment, oxidation film formation mechanism, crack growth behavior of welded joints of dissimilar metals, research gap and conclusions. In this approach the keywords were narrowed down on the influence of stainless-steel cladding on the Pressurized Water Reactor (PWR) in the nuclear plants and its impacts on warm water environments. Several published articles of relevance to this study were selected. The most relevant papers were carefully selected, evaluated and reviewed. We included studies that were published in English and reported current issues on the behavior of 308L cladding material and their effects in the nuclear plant.

Important information was extracted from the selected relevant papers and characteristics were recorded according to the research of the articles. At the end of every topic a summary of it was given and recommendation for further research on the particular topic was given as well. Finally, a conclusion containing our view and recommendation were given to future researchers.

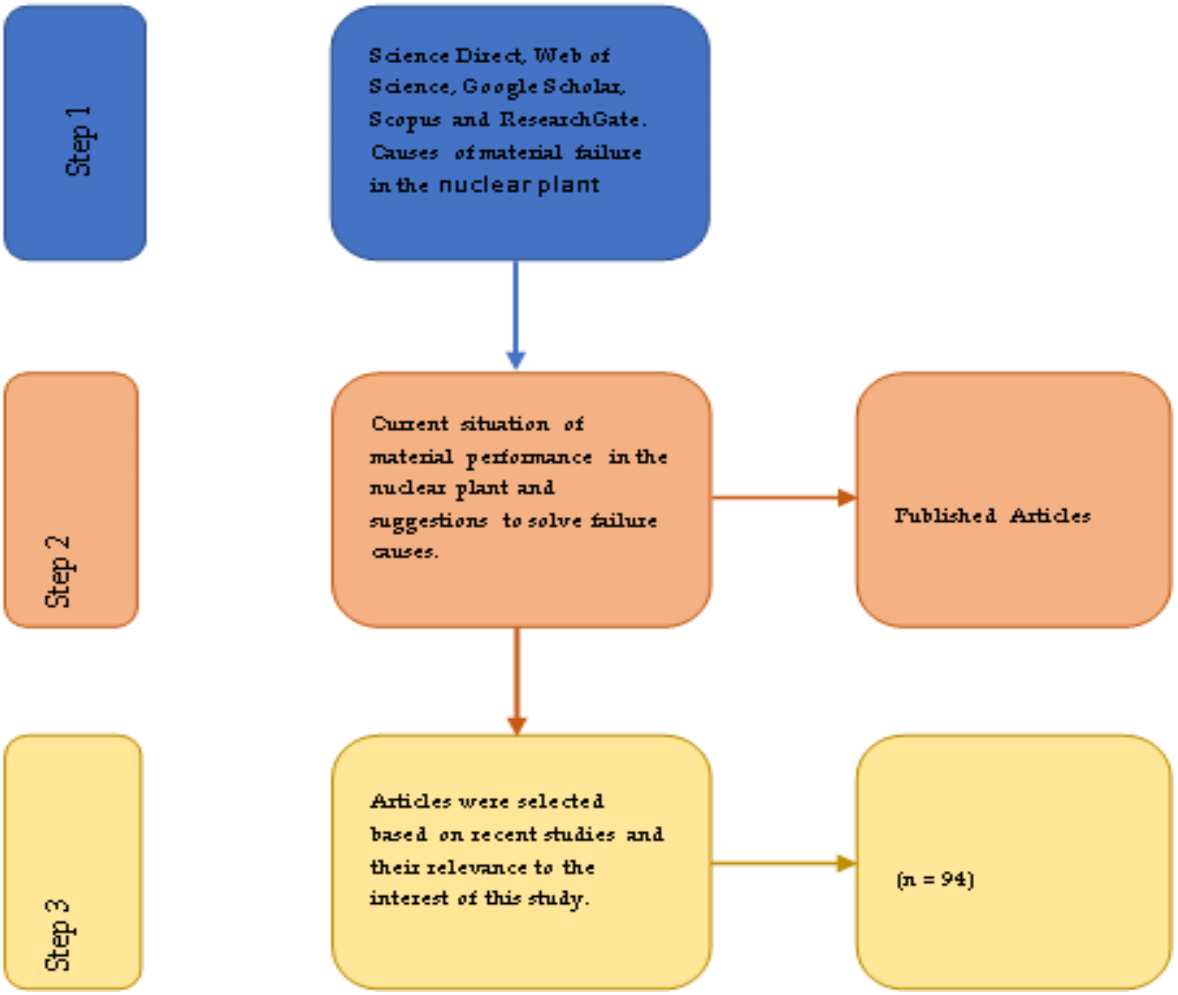

1. Introduction — Evaluation of subject by the authors
2. Methodology
   - 4 Databases (i.e. Science Direct, Google Scholar, Scopus and ResearchGate) were searched.
   - Useful articles were archived.
   - 101 articles were selected.
3. Current situation of material performance and suggestions to solve failure causes.
   In each chapter
   - Causes, simulations and the experimental analysis were stated.
   - Findings by the researchers were presented.
   - Critical analysis was done.
   - Solutions and suggestions were presented.
4. Conclusion — The authors concluded the review and air their views on influence of material performance in nuclear power plants.

3. LITERATURE REVIEW

In the reactor pressure vessel, the steam generator and the voltage regulator structural part all have a welding joint which takes over the safety end. Mn-mo-ni type low alloy steel is generally used as the connection material for the connection of the safety end with the reactor coolant pipe, which is

all made of cr-ni or cr-ni-mo austenitic stainless-steel, thus causing a welding problem of dissimilar steel.

Welding of the connection pipe and the safety end adopts surfacing welding of nickel-based alloy with a thickness of 8-10mm at the end of the connection pipe of low-alloy steel as the isolation layer. This is processed into welding groove after stress relief heat treatment and then butt joint with the safety end of stainless-steel, and no heat treatment will be carried out after welding [7].

The so-called homogeneous-heterogeneous steel welding refers to the same structure welding (austenitic steel and austenitic steel welding, ferritic steel and ferritic steel welding), such as iron based austenitic steel and nickel based austenitic steel welding which belongs to homogeneous-heterogeneous steel welding. The welding of heterogeneous steel refers to the welding of heterogeneous structure (austenitic steel and ferritic steel, ferritic steel and austenitic steel). For example, the welding between ferritic steel and ferritic austenitic steel belongs to the welding of heterogeneous steel [7].

However, in dissimilar metal welded joints, there is chemical composition, mechanical properties and structure differences, inhomogeneity and geometric discontinuity, welding process and manufacturing defects (cracks, porosity, inclusion, incomplete fusion, etc.). The complex welding thermal cycle can cause material mechanical properties and chemical composition change and generates high residual stress (RS). Pipe itself under complex loading and high or low temperature fatigue loading, also the corrosion of high temperature and high pressure water medium as well as material of irradiation embrittlement, and residual stress also serve the common role of alternating load, seriously influenced the fatigue strength of welded joint, brittle fracture resistance and resistance to stress corrosion cracking ability [8], it is easy to have between the joint an SCC and corrosion in the process [9].

Due to different materials, heterogeneous steel welding often has the following major problems:

1. The parent metal-weld metal (WM) is diluted by low-alloy and high-strength steel, and its composition and structure are quite different. At the junction between the matrix and the weld, lattice distortion will inevitably occur, which is manifested as "fusion line" on the macro level and "fusion zone" with very small size on the micro level (a narrow zone, usually 0.02~ 0.2mm wide, near the fusion line, but significant changes in composition, microstructure and hardness). Most of the damages of welded joints occur in the fusion zone, so more in-depth studies are needed on the area near the Fusion Boundary (FB).

2. Migration of chemical components in the fusion zone is mainly the diffusion and migration of carbon elements from ferrite steel to stainless-steel or nickel-based alloy.

3. Formation of welding joint cracks. In order to prevent the crack caused by quenching steel, the hydrogen-induced crack and the hot crack of the weld metal itself, in addition to selecting suitable welding materials, some elements can be added into the weld metal to partially or completely prevent the dislocation.

4. Generation of residual stress. The difference of thermal expansion coefficient and thermal conductivity between low alloy ferrite steel and high alloy austenitic steel, results in the large internal

stress at the interface. At the same time, the post-welding heat treatment temperature is in the sensitization range of stainless steel, and the residual stress is not easily removed by heat treatment.

Due to the above factors, the welded joints of dissimilar steel often fail to reach the expected life in the long service life and are prone to early failure. In view of this phenomenon, scholars from all over the world have carried out a wide range of investigation and research on the above factors in order to make clear the impact of these factors on joints.

3.1. Dissimilar metal welded joints

Reliability and integrity evaluation of welded joints is needed to ensure that the welded joints can be maintained in the whole life or extended life. Reliable integrity assessment is established on the basis of understanding of environmental action mechanism, welding joint structure, mechanical properties distribution, welding residual stress distribution, damage and fracture behavior, integrity assessment methods and so on. Only by reliable integrity evaluation can a scientific decision be made that the dissimilar metal welded joints will not be maintained and will be put into service or replaced after maintenance, so as to ensure the safe use of dissimilar metal welded joints in nuclear power plants. In view of the integrity of dissimilar metal welded joints, many researches have been carried out.

3.1.1. Microstructure dissimilar metal welded joints

Fusion zone in the welding process is by the melting of the parent metal and weld metal alloy. Generally, it can be divided into "incomplete mixing zone (Unmixed zone)" and "part of the fusion zone (partly melted zone)" of two parts, the middle of the welding interface. "Incomplete mixing zone" refers to the weld metal alloy melted during welding. The "partial melted zone" is formed by the melting of the parent metal adjacent to the weld during welding. From the perspective of crystallography, the fusion zone refers to the transition zone including the fusion line and the transition zone with crystal layer and diffusion layer. The components of this transition zone are not fixed, and the boundary between it and the base metal is called the fusion line. The crystallization layer is formed by the crystallization process of heterogeneous metals and belongs to the outer part of the fusion zone. The transition layer is formed by heterogeneous metals near the fusion line, and its composition and properties are different from those of the base metal. Transition layer formation is attributed to lattice types and metal compounds [10].

For heterogeneous metal welding, as long as the lattice types of the parent metal are the same, the crystal of the base metal and the weld fusion zone will be compatible even if the chemical composition of the parent metal is quite different. If the crystal plane spacing between the two metals is quite different, but the solid solution metal elements in the lattice can form metal compounds with each other, crystallization will also occur. At this time, a single molecular layer will appear in the fusion zone to transition from one kind of lattice to another. For the heterogeneous welded joints of fe-austenitic steel and ni-austenitic steel, because the crystallization type is fe-type, the fusion zone

compatibility of this kind of joint is good. Due to the difference in lattice size, it is inevitable to cause the lattice distortion in the transition layer at the interface, resulting in various defects of the lattice. Thereby making the compatibility of the fusion zone of this kind of joint relatively weak.

Srinivasana et al. observed the welding fusion zone of different kinds of pearlite steel and austenitic steel by high resolution transmission electron microscopy [10], and found that the structure of the fusion zone was very complex, consisting of single-phase austenite zone, austenite + martensite zone, martensite zone and fine ferrite + pearlite grain zone. Due to the welding overheating, the base material in the fusion zone often forms a heat affected zone with thick structure. The roughness of the structure leads to the decrease of toughness, and there is a large stress weld interface adjacent to the heat affected zone. In this way, the combined effect of the two factors makes the dissimilar steel joints more likely to fail than the same steel joints. Presently, heat treatment is mainly used to reduce the brittleness of joints. However, the heat treatment time needs to be controlled properly. In addition, it is necessary to improve the welding process to obtain narrow width and uniform heat affected zone in the future. In other words, heterogeneous steel welding must be based on the specific steel to take a reasonable welding process and weld filler metal so that the fusion zone has better mechanical properties

Lim [9] studied 600 alloy and 182 alloy weldments of organization and mechanical properties. The results showed that 600 alloy grain is mainly composed of a large number of twin boundary and large angle grain boundary and contains a small amount of low angle grain boundary, with large number of precipitates in grain. The 182 weld-alloy contains a large number of dendritic structures. Also, thermal gradient changes in the same direction. Srinivasana et al. [10] carried out microstructure characterization and electrochemical testing on austenitic steel-martensite steel for heterogeneous metal welds, and the results showed that the weld metal contained two-phase structure. Different structures have different effects on electrochemical corrosion behavior. Wang et al. [11] carried out microstructure characterization of the fusion interface of low-alloy ferritic steel-nickel-based alloy steels for welding of heterogeneous metals. The experimental results showed that the fusion interface of A508-alloy 52 contained two different types of fusion interfaces, type-I and type-II. The results showed that the surface potential is different in different regions and the order is V52 > V508 > V martensite.

Wu et al. [12] studied SA553-SUS304 dissimilar welded joint with different filler material ER308L and ERNiMo – 8. After the organization and the local mechanical properties, the experimental results showed the weld 304L in two phases (martensite and austenite), ERNiMo - 8 in the weld austenitic organization, only two kinds of weld organization and the component content is different, because of the laser welding cold speed leads to the different martensite with different morphology and chemical composition. At the same time, the fiber hardness at the fusion line changes due to the presence of martensite.

Ma et al. [13] investigated the microstructure changes of alloy and region of alloy 600-82 welded joints. It is found that the residual strain in the heat-affected zone close to the fusion line is very large and mainly concentrated on the grain boundary. Alloy 182-82 was investigated by Lima et al. [14] as alloy filler material for A508-316L joint. It is shown that alloy 82 has good weldability as

filler material. Tsai et al. [15] studied 182 sensitizing properties of weld metal and an experiment showed that sensitization after 24h under 650℃ is more sensitive to inter-granular corrosion.

3.1.2 Residual stress of dissimilar metal welded joints

Welding residual stress is one of the important factors for structural integrity assessment of key components and structures in nuclear power plants. Residual stress is caused by mechanical processing or heat treatment in the manufacturing process of structures or components and is affected by the elastic behavior of component materials. Therefore, residual stress existing in all engineering structural components [19] is due to residual stress component that is not under load and the initial stress on the already existing component cross section. In the process of service component and other load caused by working stress superposition mutually, it makes it to produce secondary deformation and residual stress redistribution and will seriously affect the fatigue strength of the structure. Brittle fracture resistance, resistance to stress corrosion cracking and high temperature creep cracking ability must therefore be formed on the reason of influence factors and the size as well as distribution must be studied.

In general, residual stress depends on the following key factors; material properties (structural and organizational changes), external constraints, internal constraints caused by pre-weld processing and welding process parameters (e.g., heat input, number of passes, pre-heat temperature, etc.). Relevant researches should also focus on these aspects.

According to Kloos and Kaiser [16,17], residual stress is usually generated by the interaction between the mechanics, thermal and metallurgical states of the material itself, and by the inhomogeneity of microstructure and macrostructure, such as heterogeneous metal welding, polyphase structure of metal, crystal defects or inclusions. On the other hand, the material will inevitably produce residual stress in the manufacturing process. The residual stress in service is caused by the deformation or corrosion of the material and the deformation of the crystal.

Ogawa [18] used the drilling method to characterize the residual stress distribution in the simulation parts of the safety end welding joints of PWR in each manufacturing process. The BIMET and ADIMEW projects in Europe measured the residual stress distribution in the isolation layer, welding seam and heat affected zone of the simulated dissimilar metal welding parts by neutron diffraction technology and drilling method respectively. Dike et al. [19] pointed out that it is time-consuming and costly to obtain the residual stress data of the structure through experiments, and the calculation program based on finite element can effectively solve this nonlinear problem. Killian et al. [20] numerically simulated the residual stress distribution of simulated dissimilar metal welded joints in ADIMEW project and made a comparative analysis with the test results. Lee [21] through finite element numerical analysis and test characterization of residual stress distribution in alloy 82/182 alloy welded joints. Muroya et al. [22] numerically simulated the entire manufacturing process of welded joints of dissimilar metals and obtained the residual stress distribution under each step. Deng [23] developed a simplified residual stress calculation method taking into account surfacing layer, isolation layer, post-weld heat treatment and multi-pass welding. The residual stress distribution of dissimilar

metal welded joints in nuclear power plant sfvq1a-alloy 82/ moy82-susf316 in various manufacturing stages was characterized by numerical simulation method and test method. The effects of heat source model, plating layer, isolation layer and heat treatment on the final residual stress were analyzed. Na et al. [24] studied the residual stress of dissimilar metal welded joints based on the statistical regression method

3.1.3 Mechanical properties of heterogeneous metal welding

In the process of heterogeneous metal welding, different microstructure appears in each area of the welded joint, especially in the fusion zone. This presents extremely complex structure and element distribution, making the fusion zone the most vulnerable to failure of the welded joint, thus affecting the service life of the welded structure. There have been some researches on the mechanical properties of nuclear dissimilar metal welded joints with different materials globally.

Jang et al. [25] conducted micro-tensile, hardness and fracture tests on SA508-alloy 82/182-tp316 dissimilar metal welded joints and found that there is mechanical properties inhomogeneity in both width and thickness directions of the joints. Peng et al. [26] studied 182 alloy-A533B low alloy steel dissimilar metal weld microstructure characteristics of weld zone, and found in 182 alloy welding area, fusion line interface of about 100 microns thin layer area, has the high hardness value and residual strain. There are two special grain boundary shapes, vertical and parallel to the fusion line I and Π grain boundary respectively. It puts forward the SCC in the fusion line interface extended stagnation and restart the mechanism and its interaction with water chemical condition. Finite Element Method (FEM) simulation results showed that positive hardness gradient distribution will reduce the rate of crack propagation. Hou [27, 28] points out that 182 alloy-A533B low alloy steel dissimilar metal weld crack initiation mainly in dilution zone (DZ) along the direction perpendicular to the fusion line extension, compared with type I grain boundary, type II grain boundary the unique large angle grain boundary SCC sensitivity higher, more easily become the SCC crack expansion path. Hosseini et al. [29] performed microstructure and mechanical characterization of Inconel 617/310 heterogeneous welded joints. The experimental results showed that there was no evidence of cracking in nickel-based weld metals. This conclusion is also supported by many scholars [30, 31].

Terachi et al. [32] pointed out that the yield strength of austenitic stainless-steel 316 SS and 304 SS is related to temperature and the higher the temperature, the lower the yield strength of the material. Seifert et al. [33] tested several plants with austenitic stainless-steel in the condition of different hardness on the Richter scale, Vickers hardness, yield strength and tensile strength and the curve fitting of data analysis and the regression equation between them. The Vickers hardness HV austenitic stainless steel and the relation between the material yield strength can be expressed as a linear relationship. According to the empirical formula between material hardness and yield strength, the yield strength of each area of the welded joint can be approximately obtained [35]. Hou et al. [28] using JIS test specimen and small size specimen under 288℃ respectively, 182 alloy - A533B low alloy steel in different areas of the dissimilar metal weld all yield strength were measured, and points out that the near HAZ material yield strength is higher than other three areas to 50-100 MPa. Due to

the limitation of sample location and small size, the yield strength of materials in these four areas cannot be accurately obtained. Seifer et al. [33] obtained under 288℃, 182-alloy weld the yield strength of 345 MPa. Jang et al. [34] found that the yield strength at the bottom of the 182-alloy weld was 50-70 MPa higher than that at the top.

Schwalbe [35] and Gilles [36] found that there was a high degree of heterogeneity of microstructure and mechanical properties in the local and interface area of the joint. But these studies were mainly focused on early nuclear power materials and structures. Laukkanen et al. [37] tested the fracture mechanics of SA508-E309L/E308L-AISI304 dissimilar metal welded joints by using small tensile test samples and three-point bending test samples. They pointed out that the strain in the microstructure area had a significant impact on the ductile-brittle transition and failure mode of the joints. Kim et al [38] investigated SA508Gr under room temperature and 320℃. The la-82/182-F316 SS significantly changes the local mechanical properties of dissimilar metal weld. Ming et al. [39] studied the microstructure change and local mechanical property test of SA508-309L/308L-316L heterogeneous welded joints and found that there was microstructure inhomogeneity in the fusion line of 508-alloy and 309-alloy The hardness value in the whole welded joint was constantly changing.

The inhomogeneity of mechanical properties of welded joints (i.e. the mismatch between the base metal and the strength of the weld metal) has a great influence on the stress distribution characteristics and the constraint state near the crack tip of the weld. It is also the essential reason why the strength and fracture behavior of welded joints are different from that of homogeneous materials. Boothmnan et al. [40] found that the concentration of plastic constraint in weld material resulted in the increase of J-integral of low-match weld crack. The concentration of the plastic constraint on the base metal results in the decrease of the J-integral of the weld crack with high matching. Yang et al. [48] showed that the stress state of the leading edge of type I crack of welded joint sample had obvious plane strain characteristics. The stress triaxiality only reached the maximum value near the ligament and the matching degree of joint was the main factor leading to the change of triaxial stress constraint of welded joint. Kim et al. [41, 42] found that the stress triaxiality of the softer side of the crack at the junction of the weld and the base metal was greater than that of the crack in the same soft homogeneous material. Dumerval et al. [49] research on three-point bending crack samples showed that the plastic zone of low-match welded joints was small and was restrained in the weld, while the plastic zone of high-match welded joints was large and extended to the base metal. Lu et al. [50] carried out an experiment on the J-integral of the crack in the weld zone of the high-match welding joint. With the decrease of matching ratio, the strain in this region becomes more concentrated, while the weld deformation decreases and the driving force of crack growth increases. Hong et al. [43] used notched tensile specimens to study the effects of highly matched welded joints on the fracture strain of welds and base metals, stress triaxiality at fracture, and critical hole expansion ratio. Hong et al. [43] studied the influence of initial crack location, depth, strength mismatch, crack resistance and propagation path between different materials on the welding joints of dissimilar metals. Uyulgan [44] found that weld crack of dissimilar metal welded joint has small crack growth resistance and base metal crack has high crack growth resistance. Itatani's [45] study on the local fracture performance of dissimilar metal weld tested 182-alloy and 82 fracture toughness of the alloy at room temperature and 300℃ high temperature. Samal [46] pointed out that the interface between the isolation layer and the

weld seam was the weak position of the dissimilar metal welded joint, where the crack growth resistance was low. Ogawa et al. [47] studied cracks in the fusion line, with the crack propagation, dissimilar metal weld J-Δ a curve from the J-182 alloy Δ SQV2A a curve to the homogeneous materials.

3.1.4 Corrosion performance of Stainless-steel welding parts

In the welding process of stainless-steel, because various factors may appear in the welding joint, such as porosity, segregation, crack, embrittlement or inclusion defects, so also in the austenitic stainless-steel welding joint in the service environment often appear the uniform corrosion, pitting corrosion, intergranular corrosion and stress corrosion and other corrosion behaviors.

I. UNIFORM CORROSION

When stainless-steel and other nuclear structural materials are in service in high-temperature and high-pressure water environment, uniform corrosion will occur, that is, oxidation behavior. It is the most basic form of corrosion, and also the basis of other environmental failure processes such as stress corrosion (SCC). Martin et al. [53] compared and studied the oxidation behavior of martensitic steel (EM10 and T91, etc.) and austenitic steel (American standard 316L and 304L), and found that there was a critical temperature for corrosion, especially for 304L stainless-steel. All materials were corroded except 304L stainless-steel after 3000h. The excellent corrosion resistance of stainless-steel is mainly attributed to the protective oxide film formed on its surface in the corrosive medium. Gao [65] pointed out that the chemical and physical properties of the corrosion product film formed in high temperature and high-pressure water play an important role in the corrosion fracture process of the material environment, especially in the initial stage of fracture.

Ziemniak [54] studied the cross-section morphology and structure of oxide film generated by 304L and 316L stainless-steel series in high-temperature and high-pressure water containing oxygen and hydrogen. It was found that the oxide film was a double-layer structure and the outer layer was composed of monocrystalline large particle oxides, mainly fe-rich oxides with poor protection. The inner layer is composed of dense polycrystalline fine grains, mainly rich in Cr oxides, which can effectively inhibit the further corrosion of the metal. Some scholars [68, 69] studied the composition and structure of the oxide film of 304L stainless-steel corroded by high-temperature pure water, and found that the oxide film was divided into three layers; upper porous layer, middle cracked layer and inner insulating layer, which effectively prevented corrosion. However, most studies show that the oxide film formed by stainless-steel is a double layer structure.

II. PITTING

Pitting is concentrated in a small area on the metal surface and penetrates into the pitted hole of the metal. The corrosion hole is usually small and deep in diameter, which is one of the corrosion forms with destructive and hidden dangers. Pitting corrosion is usually caused by some defects on the

metal surface. The tendency of pitting corrosion occurs in welding joints due to segregation of chemical elements such as Cr, uneven chemical composition in the fusion zone, and difference in structure and performance in the heat-affected zone due to uneven heating. The main conditions for pitting corrosion of materials are as follows; (1) it occurs mainly on metal materials with passivation film generated on the surface or on metals with negative polarity coating on the surface; (2) it occurs in the medium with special ions. Generally speaking, stainless-steel is particularly sensitive to halogen ions. These anions are not evenly adsorbed on the surface of the alloy, resulting in the uneven destruction of the passivation film; (3) pitting corrosion generally occurs above a critical potential, which is called pitting potential [70].

III. INTERGRANULAR CORROSION

Intergranular corrosion refers to the local damage caused by the action of micro batteries in some environments where the physical and chemical state of the grain boundary is different from that inside the grain. It is a kind of local corrosion with great harm. The mechanism of intergranular corrosion is the theory of poor chromium. Poor chromium theory is originally found in austenitic stainless-steel because most of the austenitic stainless-steel after solid solution treatment, at more than 0.03% when the content of carbon in steel and used in sensitization temperature or heat treatment, C is part or all of the supersaturated precipitation from austenite, formation of chromium carbide (mainly Cr23C6) and continuous distribution on the grain boundary. In the precipitation process, the diffusion resistance of carbon is small and can reach the grain boundary quickly, while the diffusion resistance of chromium in the austenite is large. So, when the carbide is formed, the chromium near the grain boundary must be consumed in order to form a chromium poor area (chromium content less than 12%) near the grain boundary and then produce inter-crystalline corrosion [73, 74].

Zhang et al. [84] studied the intergranular corrosion behavior of 316L. The experimental results showed that sensitized heat treatment would aggravate the intergranular corrosion degree of 316L stainless-steel, and the width of intergranular corrosion groove increased with the increase of sensitized heat treatment time. The influence of heating temperature and time on the intergranular corrosion of austenitic stainless-steel is shown in figure 2-3. Rhouma et al. [58] studied the effect of 316L structure and phase composition on intergranular corrosion, and the results showed that sensitization and desensitization were still controlled by the chrome-poor region around the austenite grain boundary. The remaining ferrite and composition had no significant influence on the corrosion behavior of 316L with 1%-fe.

IV. STRESS CORROSION

Stress corrosion (SCC) occurs mostly at welded joints of stainless steel. Stress corrosion cracking of stainless steel refers to a kind of cracking phenomenon that occurs under the combined action of static tensile stress, sensitive materials and specific corrosive media of stainless-steel. This kind of corrosion occurs in a short time and is extremely destructive. Stainless-steel in the water solution containing oxygen chloride ions, first in the metal surface form an oxide film that prevents the corrosion for stainless-steel passivation. Due to the tensile stress of the pressure vessel itself and the

additional stress caused by the thickening of the protective film, the protective film in the local area is cracked, and the base metal at the crack is directly exposed to the corrosive medium. The electrode potential there, is lower than the intact part of the protective film, forming the anode of the micro batteries and producing anodic dissolution. The fact that the anode is small, and the cathode is large, the dissolution rate of the anode is high. After the corrosion reaches a certain degree, a new protective film is formed. However, under the action of tensile stress, it can be destroyed again, and new anodic dissolution occurs. In the process of repeated formation and rupture of the protective film, the corrosion in some local areas will deepen and finally form holes, and the existence of holes will cause stress concentration, and accelerate the plastic deformation of the surface of the holes and the rupture of the protective film. This joint action of tensile stress and corrosive medium results in stress corrosion cracks [77, 78].

Terachi [61] studied the cause of stress corrosion cracking of 316L stainless-steel. The wedge-shaped force of oxidation caused by corrosion causes local tensile stress at the tip, which can promote crack initiation and propagation. Corrosion products, mainly Fe3O4, were present in the crack, while the crack tip was rich in Cr oxides and the Ni-rich products were at the front end of the crack tip.

Corrosion product films in high-temperature and high-pressure water environment

Presently, most papers describe the two-layer structure of the oxide film formed in high-temperature and high-pressure water environment; the inner layer is rich in Cr layer, which is composed of a large number of Cr rich spinel structure oxides, and the outer layer is large size Fe rich oxides (stainless-steel) or Ni rich oxides (ni-based alloy).

Terachi et al. [64] studied the cross-section morphology and structure of the oxide film generated by cold-processed 316L stainless-steel in simulated PWR water, and found that the oxide film was of double-layer structure, the outer layer was composed of single crystal particles, with a thickness of about 1~2 m. The inner layer was composed of polycrystalline fine grains with a thickness of about 500nm. By Energy Dispersive Spectrometer (EDS) line scanning analysis results, outer layer is mainly composed of Fe oxides lining for Cr oxide.

Meanwhile, Terachi [64] also studied the section morphology and structure of the oxide film generated by nickel-based alloy 600 in simulated PWR water, and found that the oxide film also has a two-layer structure, with the outer layer composed of needle-like oxides and the inner layer composed of nanocrystals. The oxidation mechanism is presented as shown in figure 3-4. Indicating that the morphology and density of surface oxides have a great influence on the oxidation degree of nickel-based alloys.

Teysseyre [65] studied 316L/SS at temperatures higher than 395℃ for 24MPa pressure without oxygen supercritical deionized water generated in the cross-section morphology of oxidation film. The results found that it is not easy to see the morphology of the thin oxide film layer (about 10 microns). Due to the limitations of equipment and experimental conditions, few studies and reports have been carried out on the cross section of oxide film and further studies are needed.

Effects of artificial aging heat treatment on corrosion behaviour and mechanical properties of AA6XXX alloy was discussed by Onat [92]. Increase in aging time results in an increase in mechanical properties of the material and the corrosion resistance is determined by the artificial aging

time as indicated by experimental results. At a temperature of 190℃ and 10-h aging period, the best corrosion resistance value was obtained.

The effects of thermal aging on localized corrosion behavior of lean duplex steel (LDSS 2404) between temperatures 650 and 850℃ was investigated by Zanotto et al [93]. Using Optical Method (OM) and Scanning Electron Microscopy (SEM) with Focused Ion Beam (FIB) integrated to SEM, they studied intergranular corrosion (IGC) attack after double loop electrochemical potentiokinetic reactivation (DL-EPR). Nitride precipitation was caused mainly by aging at 650℃ or 5minutes aging time at 750℃, at α/α grain boundaries and is due to fast diffusion of chromium in the phase, as observed by the study. Aging allowed precipitation at α/ϒ interface at 850℃ or 10-60 minutes at 750℃. The study concluded that pitting attack only affected the α-phase based on electrochemical tests conducted. Also, in aged samples, pitting and IGC attack were detected near the nitrides in correspondence of α/α and α/ϒ grain boundaries depending on aging temperatures and times.

Koyanbayev et al [94] conducted a forecast estimation of anticipated corrosion damage of boundary material at the radionuclide released from burnt fuel assemblies of BN-350 reactor into the environment during dry storage for 50 years. The study concluded that corrosion damage to material is not dangerous at standard storage conditions as indicated by the forecast data for the corrosion damage of the fuel element cladding at the release of the radioactive fission products into the environment for 50 years of dry storage of the reactor FA. Also the barrier material's depth of destruction during the entire period of dry storage shall not exceed 3 μm, but corrosion layer depth can reach 25 μm under emergency dry storage of fuel assembly conditions. This significantly increases probability of barrier material's corrosion cracking.

Zhu et al [95] employed Scanning Electron Microscope (SEM) to study the microstructures evolution of precipitations for ultra-low iron alloy 625 subjected to long term aging treatment at 750℃. ASTM G28A was used to evaluate the intergranular corrosion behaviours of Alloy 625. The investigation concluded that during aging treatment, corrosion resistance of Alloy 625 was greatly reduced. Dissolution of precipitated phase and chromium depleted zone was the cause of the decrease in intergranular corrosion resistance of Alloy 625. Johnson-Mehl-Avrami equation can be used to simulate the volume of precipitated phase which is related to the mass loss rate of Alloy 625 after aging treatment.

V. OXIDATION FILM FORMATION MECHANISM:

There are not many studies on the growth mechanism of oxide film in high temperature water. Only two typical models are available as follows;

I. Both the inner and outer layers of the oxide film are formed by solid state growth, which is Robertson's model inferred from the similarity of oxide growth in hot steam and hot water. According to the model, the growth of the inner layer of the oxide film on the surface of stainless-steel is due to the effect of water passing through the oxide pores. According to the diffusion rate of metal ions in the spinel lattice, Cr and Ni migrate more slowly than Fe and thus the inner layer is enriched. The growth of the outer layer is mainly diffused along the oxide boundary by iron ions. According to this model, the literature [82, 83] on PWRS 316L stainless-steel at 320℃ in the simulation of water generated by

the oxidation film of EDS analysis results accords well with the results of the model analysis. It can be seen that this model can explain the growth process of some materials, such as austenitic stainless-steel oxide film in hot water [84-86].

II. The inner and outer layers of the oxide film are formed by metal dissolution and oxide precipitation. This is the oxide growth model proposed by Winkle. In literature [89-93] modified 304L stainless-steel in the high temperature of 288°C and 9MPa pure water (dissolved oxygen concentration for 2 x 10-6 parts per million (PPM) in the formation of the oxide film. For example, a brief introduction of the model; in high temperature water, stainless-steel dissolved in stomatal activity at the bottom of the location, the concentration of dissolved metal elements increase made the position of the spinel oxides sedimentation possible. The mixed oxides were precipitated from the components of stomatal solution according to the order of their formation free energy. At the same time, the concentration gradient of dissolved metal ions between the active corrosion site and the outer/aqueous phase boundary causes the outward diffusion of metal elements through the pores. A portion of the outward diffusion precipitates as a thin lamellar boundary of the inner oxide in the form of Fe3O4 or mixed spinel, leading to the formation of an outer oxide layer of coarse grains. This explains why the outer particles of the generated oxide film are larger and the inner particles are smaller [92-93].

The above description of Robertson's model and Winkler model indicates that both models can basically explain the properties of oxide film formed by some materials such as austenitic stainless-steel in hot water. Comparing the two models, it is found that Robertson model and Winkler model are mainly using the diffusion principle. Robertson model is analyzed from the angle of the rate of diffusion and the Winkler model from the angle of free energy analysis. The former well explained the oxide film inner rich Cr outer rich Fe phenomenon, which explains the outer layer of the oxide film grain is bulky, inner particles are relatively small. Another model is a combination of Robertson's model, which explains the growth of the inner layer and Winkler's model which describes the formation of the outer layer.

3.1.5 Crack growth behavior of welded joints of dissimilar metals

The experimental and numerical simulation studies on the damage and fracture behavior of laboratory specimens of dissimilar metal welded joints mainly include the corrosion fatigue mechanism and performance studies of related joint materials. The experimental analysis of tensile and fracture toughness of materials and the simulation of ductile damage and fracture behavior of cracks by local methods [82, 83] and Gurson-Needleman-Tvergaard (GTN) model [82-85]. Samal [86] simulated the fracture resistance and fracture behavior of welded joints of nuclear heterogeneous metals by local method and believed that the driving force of crack tip depended on the location of the initial crack, and the crack could expand in any material. Bourgeois et al. [87] simulated the crack growth by using the Rousselier model of local method and concluded that the interface of nickel-based alloy/ferritic steel is the weakest region of the welded joints of heterogeneous metals. In SINTAP, ESIS, ASTM and other assessment methods, the solution of local fracture parameters is also described. At the same time, it is pointed out that if the local method is applied to the brittle fracture assessment of actual structures, a large number of studies need to be done [88].

The deformation behavior of different microstructures has different effects on the mechanical properties of materials. Therefore, understanding the microstructure characteristics is helpful to optimize the mechanical properties of steel. To date, only a few studies on in-situ tensile testing of welded joints by heterogeneous welding have been reported. Roach [89] tested nickel-based alloy and nitrogen-stabilized austenitic steel by in-situ EBSD technique and found that the cracks formed preferentially at the annealing twin boundary of nickel-based stainless steel. Kim, et al. [41] studied SA508Gr under room temperature and 320℃. The la-82/182-F316 SS significantly changes the local mechanical properties of dissimilar metal weld found in the heat affected zone with the smallest plastic which is also the easiest to crack initiation. Zhang et al. [84] studied the theory of crack initiation and propagation at the twin boundary. They analyzed the principle of crack propagation at the twin boundary by using dislocation stacking energy and proposed a theoretical model of dislocation leading to crack propagation at the twin boundary, as shown in fig. 3-5.

Wang [88] studied the local mechanical properties of alloy 52M heterogeneous welding with small-size samples and found that the local mechanical properties were different in the fusion line area. Wang [88] also studied the fracture properties of heterogeneous weldment A508 ferritic steel/Alloy52M/316LSS and the results showed that the crack generally expanded from the fusion zone and heat affected zone to the inner part of the metal. Jang [92] studied the effect of microstructure and residual stress on the crack growth of welding parts, and the results showed that the residual stress caused the crack to expand preferentially on the austenite dendritic boundary, and the crack to expand rapidly at the bottom of welding seams with high residual stress. Das [93] et al. studied the tensile properties of 301L stainless-steel by in-situ stretching and the results showed that the grain containing two kinds of slip surfaces would undergo tissue transformation in the biaxial stretching process.

3.2. Research Gaps

From the above analysis, it can be seen that there are many global researches on the microstructure, microstructure and mechanical characterization, fracture behavior and other aspects of different metal welded joints. However, there are still problems that need further analysis and research as follows:

1. Presently, there are few related literatures on the microstructure of 316L stainless-steel /Inconel 182-alloy of dissimilar welded joints and microstructure of the welded joints are still not clear. At the same time, due to the complexity of welding joint structure, there are different types of fusion lines, and the related literature lacks the understanding and exploration of the reasons for the formation of different types of fusion lines.
2. Different microstructures in different areas of welded joints have different effects on distribution of components, microhardness, surface potential and residual strain, etc. Presently, the research on the influence of 316LSS/Inconel 182 weldment microstructure on the corrosion tendency of weldment has not been fully understood.
3. Due to the complexity of the structure of welded joints, there are relatively few studies on the oxidation mechanism of welded joints under high temperature and pressure water environment,

especially on the oxidation mechanism of different types of fusion interfaces. The influence of the structure of different types of fusion interfaces on the oxidation mechanism is still unclear.

4. There is a lack of in-depth research on the influencing factors of deformation behavior and micro-fracture mechanism of different parts of heterogeneous welded joints. The effect of microstructure evolution and other behaviors on fracture mechanism in the tensile process has not been studied in-depth Subheadings

4. CONCLUSION

Dissimilar metal welding is the key part of the nuclear power main safety end. Due to the complexity of the dissimilar metal welding organization and micro fracture mechanism, its security and stability determine the normal operation of the plant. The relationship between the high temperature corrosion mechanisms is still not clear. It cannot effectively support dissimilar metal weld and the establishment of the structural integrity analysis of advanced technology. Therefore, it is of great significance to study more and explore the microstructure and corresponding performance characteristics of complex heterogeneous metal welded joints for improving the service life of the welding area. At the same time, it can provide some references for the development of new nuclear power pipeline materials and new welding technology.

References

1. Q.J. Peng, T. Shoji, H. Yamauchi, *Corrosion. Science*, 49 (2007) 2767.
2. J.W. Kim, K. Lee, J.S. Kim, T.S. Byun, *J. Nucl. Mater*, 384 (2009) 212.
3. P. Riccardella, *Proceedings of International Seminar on Welding and Non-Destructive Examination in Nuclear Power Plants*, 2009, Suzhou, China. CD-ROM.
4. Y.C. Lu, *Material Degradation & Chemical Control Training Course for SG Life Management*, 2007, Suzhou, China. CD-ROM
5. S. Findlan, *Proceedings of International Seminar on Welding and Non-Destructive Testing in Nuclear Power Plants*, 2009, PE-IWE. CD-ROM.
6. C. Jang, J. Lee, and Kim J S, *International Journal of Pressure and Piping,* 85 (2008) 635.
7. P.M. Scott, *Corrosion. Science*, 25 (1985) 583.
8. Y.S. Lim, H.P. Kim, and H.D. Cho, *Mater. Charact.*, 60 (2009) 1496.
9. P.B. Srinivasana, M.P.S. Kumarb. *Mater. Chem. Phys.*, 115 (2009) 179.
10. S.Y. Wang, J Ding and H.L. Ming, *Mater. Charact.*, 100 (2015) 50.
11. Y. Wu, Y. Cai, H. Wang and S.J. Shi, *Mater. Des.*, 87 (2015) 567.
12. C. Ma, J.N. Mei and Q.J. Peng, *J. Mater. Sci. Technol.*, 31 (2015) 1011.
13. L.I.L Lima, A.Q. Bracarense and A.R.A. Chilque, *20th International Congress of Mechanical Engineering*, 2009 Gramado, RS, Brazil.
14. W.T. Tsai, C.L. Yu, J.I. Lee, *Scr. Mater.*, 53 (2005) 505.
15. K.H. Kloos, and B. Kaiser, *DGM Informationsgesellschaft mbH, Oberursel.* 22 (1991) 205.
16. K.H. Kloos, *Zeitschrift für Werkstofftechnik,* 10 (1979) 293.
17. K. Ogawa, L.O. Chidwick and E.J. Kingston, *Proceedings of ASME 2009 Pressure Vessels and Piping Division Conference*. Prague, Czech Republic. July 26-30, 2009. PVP2009-77830.
18. J. Dike, C. Cadden and C. Corderman, *International Trends in Welding Research*. ASM International, Materials Park, Ohio. 1996, 57-66.
19. D.E. Killian and S.H. Mahmoud, *Proceedings of 2008 ASME Pressure Vessels and Piping Division Conference*. Chicago, Illinois, USA. July 27-31, 2008. PVP2008-61642

20. K.S. Lee, W. Kim and J.G. Lee, *J. Mech. Sci. Techno,* 23 (2009) 2948.
21. I. Muroya, Y. Iwamoto and N. Ogawa, *Proceedings of 2008 ASME Pressure Vessels and Piping Division Conference*. Chicago, Illinois, USA. July 27-31, 2008. PVP2008-61829
22. D. Deng,S. Kiyoshima and K. Ogawa, *Nucl. Eng. Des,* 241 (2011) 46.
23. M.G. Na, J.W. Kim and D.H. Lim, *Nucl. Eng. Des,* 238 (2008) 1503.
24. C. Jang, J. Lee and J. Sung Kim, *Int. J. Press. Vessels Pip*, 85 (2008) 635.
25. Q. Peng, H. Xue and J. Hou, *Corros. Sci.,* 53 (2011) 4309.
26. J. Hou, Q.J. Peng and Y. Takada, *Corrosion. Sci.,* 52 (2010) 3949.
27. J. Hou, Q.J. Peng and Y. Takeda, *J. Mater. Sci.,* 45 (2010) 5332.
28. H.S. Hosseini, M. Shamanian and A. Kermanpur, *Mater. Charact.,* 62 (2011) 425.
29. S.Y. Wang, J. Ding and H.L. Ming, *Mater. Charact,* 100 (2015) 50.
30. Y.S. Lim, H.P. Kim and H.D. Cho *Mater. Charact,* 60 (2009) 1496.
31. T. Terachi, T. Yamada and Miyamoto, *J. Nucl. Sci. Techno,* 45 (2008) 10.
32. H.P. Seifert, S. Ritter and T. Shoji, *J. Nucl. Mater,* 378 (2008) 197.
33. C. Jang, J. Lee and J. Sung Kim, *Materials Design,* 31 (2010) 1862.
34. K.H. Schwalbe, A. Cornec and D. Lidbury, *Int. J. Press. Vessels Pip.,* 81 (2004) 251.
35. P. Gilles, J. Devaux and M.F. Cipière, *ASME 2004 Pressure Vessels and Piping Conference*, 2004: 37-54.
36. A. Laukkanen, P. Nevasmaa and U. Ehrnsten, *Nucl. Eng. Des*, 237 (2007) 1.
37. J.W. Kim, K. Lee and J.S. Kim *J. Nucl. Mater,* 384 (2009) 212.
38. H.L. Ming, Z.M. Zhang and J.Q. Wang, *Mater. Charact.*, 97 (2014) 101.
39. D.P. Boothman,M.M.K. Lee, A.R. Luxmoore, *Eng. Fract. Mech*, 64 (1999) 433.
40. Y.J. Kim and K.H. Schwalbe, *Eng. Fract. Mech*, 71 (2004) 1177.
41. J.J. Kim, S.H. Kim and K.J. Choi, *J. Corros. Sci. Eng*, 86 (2014) 295.
42. J.D. Hong, C.H. Jang and T.S. Kim. *Int. J. Fatigue*, 82 (2016) 292.
43. B. Uyulgan, H. Cetinel. *J. Mech. Sci. Technol*, 25 (2011) 2171.
44. M. Itatani, T. Saito and T Hayashi, *ASME 2009 Pressure Vessels and Piping Conference*, 2009: 419-427.
45. T. Ogawa, M. Itatani and T. Saito, *Int. J. Press. Vessels Pip.*, 90 (2012) 61.
46. Y. Xie, Y.Q. Wu and J. Burns, *Mater. Charact.*, 112 (2016) 87.
47. M. Dumerval, S. Perrin and L. Marchetti, *Corrosion Science*, 107 (2016) 1.
48. Z. Lu , J. Chen and T. Shoji, *J. Nucl. Mater*, 458 (2015) 253.
49. H.C. Wu, B. Yang, and S.L. Wang, *Mater. Sci. Eng. A*, 633 (2015) 176.
50. H. Ming, Z. Zhang and J. Wang, *Appl. Surf. Sci.*, 337 (2015) 81.
51. F.J. Martın, L. Soler and F. Hernandez, *J. Nucl. Mater*, 335 (2004) 194.
52. S.E. Ziemniak, M. Hanson and P.C. Sander, *Corrosion Science*, 50 (2008) 2465.
53. W. Kuang, X. Wu and E.H. Han, *Corrosion Science*, 52 (2010) 4081.
54. J. Lehmusto, B.J. Skrifvars and P. Yrjas, *Fuel Process. Technol.*, 105 (2013) 98.
55. A.B. Rhouma, T. Amadou and H. Sidhom, *J. Alloys Compd.*, 708 (2017) 871.
56. Z. Zhai, H. Abe and Y. Miyahara, *Corrosion. Science*, 92 (2015) 32.
57. M. Turski, and L. Edwards, *Int. J. Press. Vessels Pip.*, 86 (2009) 126.
58. T. Terachi, K. Fujii and K. Arioka, *J. Nucl. Sci. Technol.*, 42 (2005) 225.
59. S. Lozano-Perez, K. Kruska and I. Iyengar, *Corrosion. Science*, 56 (2012) 78.
60. K. Arioka, T. Yamada and T. Miyamoto, *17th International Conference on Environmental Degradation of Materials in Nuclear Power Systems – Water Reactors* August 9-12, 2015, Ottawa, Ontario, Canada.
61. T. Terachi, N. Totsuka and T. Yamada, *J. Nucl. Sci. Technol.*, 40 (2003) 509.
62. S. Teysseyre and G.S. Was, *Corros. Sci.*, 40 (1998) 337.
63. M. Dumerval, S. Perrin and L. Marchetti L, *Corrosion. Science*, 107 (2016) 1.
64. Y. Cui, S. Liu and K. Smith, *Adv. Water. Res.*, 88 (2016) 816.

65. J. Umeda, N. Nakanishi and K. Kondoh, *Mater. Chem. Phys.*, 179 (2016) 5.
66. Y. Xie, Y. Wu and J. Burns, *Mater. Charac.*, 112 (2016) 87.
67. L. Marchetti, S. Perrin and F. Jambon, *Corrosion. Science*, 102 (2016) 24.
68. Y. Cui, S. Liu and K. Smith, *Water. Res.*, 88 (2016) 816.
69. H. Xu, L. Wang and D. Sun, *Appl. Surf. Sci*., 351 (2015) 367.
70. Y. Xie, Y. Wu and J. Burns, *Mater. Charact.*, 112 (2016) 87.
71. M. Mozetič, A. Vesel and J. Kovač, *Thin Solid Films*, 591 (2015) 186.
72. L. Jinlong, L. Hongyun and L. Tongxiang, *J. Nucl. Mater.*, 466 (2015) 154.
73. H. Xu, L. Wang and D. Sun, *Appl. Surf. Sci.*, 351 (2015) 367.
74. S.Y. Persaud, S. Ramamurthy and R.C. Newman, *Corrosion. Science*, 90 (2015) 606.
75. X. Cheng, Z. Jiang and D. Wei, *Surf. Coat. Techno.*, 258 (2014) 257.
76. F.M. Beremin, *Metallurgical Transactions A*, 12A (1981) 723.
77. F.M. Beremin, A. Pineau and F. Mudry, *Metall. Trans. A.*, 14 (1983) 2277.
78. W, L, H. Gao and H. Nakashima, *Mater. Charac.*, 118 (2016) 431.
79. S. Sinha, J.A. Szpunar and N.A.P Kiran Kumar, *Mater. Sci. Eng., A*, 637 (2015) 48.
80. S. Zhang, P. Wang and D. Li, *Mater. Sci. Eng., A*, 635 (2015) 129.
81. A. Stratulat, J.A. Duff and T.J. Marrow, *Corrosion. Science*, 85 (2014) 428.
82. M.K. Samal, K. Balani and M. Seidenfuss, *J. Mech. Eng. Sci.*, 223 (2009) 1507.
83. M. Bourgeois, O. Ancelet and S. Marie, *ASME 2012 Pressure Vessels and Piping Conference*, 2012: 437-444.
84. H.T.Wang, G.Z.Wang and F.Z. Xuan, *Advanced Materials Research*, 509 (2012) 103.
85. M.D. Roach, S.I. Wright and J.E. Lemons, *Mater. Sci. Eng. A*. 586 (2013) 382.
86. H.T. Wang, G.Z. Wang and F.Z. Xuan, *Mater. Sci. Eng. A*. 568 (2013) 108.
87. H.T. Wang, G.Z. Wang and F.Z. Xuan, *Eng. Fail. Anal*. 28 (2013) 134.
88. C. Jang, P.Y. Cho and M. Kim, *Mater. Des*. 31 (2010) 1862.
89. Y.B Das, A.N. Forsey and T.H. Simm, *J. Comput.-Aided Mater. Desc.*, 112 (2016) 107.
90. S. Chakrabarty, S.K. Mishra, P. Pant, *Mater. Sci. Eng. A*. 617 (2014) 228.
91. A. Onat, *J. Chem. Eng*. and *Mat. Sci.*, 9 (2018) 17.
92. F. Zanotto, V. Grassi, A. Balbo, F. Zucchi and C. Monticelli, *Metals*, 9 (2019) 529.
93. Y. T. Koyanbayev, M.K. Skakov, E.G. Batyrbekov, I.I. Deryavko, Y.Y. Sapatayev and Y.A. Kozhahmetov, *Sci. Technol. Nucl. Install*, 2019 (2019), 9.
94. Z. Zhu, Y. Sui, A. Dai, Y. Cai, L. Xu, Z. Wang, H. Chen, X. Shao and W. Liu, *Int. J. Corros*., 2019 (2019) 9.